NASA TECHNICAL NOTE

NASA TN D-5692

NASA TN D-5692

XB-70 COMPRESSOR-NOISE REDUCTION AND PROPULSION-SYSTEM PERFORMANCE FOR CHOKED INLET FLOW

by Terrill W. Putnam and Ronald H. Smith

Flight Research Center
Edwards, Calif.

NATIONAL AERONAUTICS AND SPACE ADMINISTRATION • WASHINGTON, D. C. • MARCH 1970

1. Report No.	2. Government Accession No.	3. Recipient's Catalog No.
NASA TN D-5692		

4. Title and Subtitle	5. Report Date
XB-70 COMPRESSOR-NOISE REDUCTION AND PROPULSION-SYSTEM PERFORMANCE FOR CHOKED INLET FLOW	March 1970
	6. Performing Organization Code
7. Author(s)	8. Performing Organization Report No.
Terrill W. Putnam and Ronald H. Smith	H-578
	10. Work Unit No.
9. Performing Organization Name and Address	720-51-00-05-24
NASA Flight Research Center P. O. Box 273 Edwards, California 93523	11. Contract or Grant No.
	13. Type of Report and Period Covered
12. Sponsoring Agency Name and Address	Technical Note
National Aeronautics and Space Administration Washington, D. C. 20546	14. Sponsoring Agency Code

15. Supplementary Notes

16. Abstract

An investigation was conducted with the XB-70 airplane attached to a thrust stand to observe compressor-radiated noise and propulsion-system performance as the inlet throat area was reduced to form an aerodynamically choked flow. The anticipated compressor-noise reduction was not experienced. Tests at constant engine speed settings disclosed only minor noise reductions as a result of choking the inlet. Additional tests were performed with the inlet fixed full open and the engines set at successively higher speeds from 60-percent to 87-percent rpm. These tests disclosed considerable noise reduction (10 decibels) in the compressor-blade passing frequencies at engine settings above 80-percent rpm. Thus, it was concluded that most of the noise reduction expected for the throat-closing tests, which were done at engine settings of 87-percent rpm and higher, had already occurred and that only slight additional suppression could be expected when the throat area was decreased to choke the flow.

Choking the flow resulted in thrust losses due to decreased total-pressure recovery and airflow in the inlet. These test results suggest that major noise reduction may be obtained without a full-choked flow and the concurrent propulsion-system performance loss.

17. Key Words Suggested by Author(s)	18. Distribution Statement
Inlet choking - Noise suppression - Propulsion-system performance - XB-70 airplane	Unclassified - Unlimited

19. Security Classif. (of this report)	20. Security Classif. (of this page)	21. No. of Pages	22. Price *
Unclassified	Unclassified	25	$3.00

*For sale by the Clearinghouse for Federal Scientific and Technical Information, Springfield, Virginia 22151.

XB-70 COMPRESSOR-NOISE REDUCTION AND PROPULSION-SYSTEM PERFORMANCE FOR CHOKED INLET FLOW

By Terrill W. Putnam and Ronald H. Smith
Flight Research Center

INTRODUCTION

Aircraft engine noise in the vicinity of populated areas, and particularly near airports, has become an increasingly severe problem. The problem of noise suppression has been attacked in recent years through many alleviation techniques. The techniques have ranged from developing quieter engines to acoustically treating engine nacelles (ref. 1) and altering aircraft flight paths, operating procedures, and propulsion-system geometries (refs. 1 and 2). One of the latter techniques involves the application of variable inlet geometry to aerodynamically choke the inlet. References 3 to 5 discuss results obtained by choking subsonic inlets.

Most supersonic aircraft, because of their wide speed ranges, must incorporate variable-geometry inlets to match inlet capabilities to engine airflow requirements. The variable-geometry feature of such an inlet raises the possibility of choking the inlet for noise suppression during landing. However, supersonic inlets typically have sharp leading edges for high-speed operation that can grossly affect inlet airflow at subsonic speeds. The effects of both inlet choking and sharp leading edges were studied at the NASA Langley Research Center where researchers operated a small turbojet engine connected to a supersonic inlet (ref. 6). Aerodynamic choking of the inlet flow was induced and the resultant noise suppression and propulsion performance measured. Noise suppression in the compressor-blade passing frequencies was observed to be as high as 20 decibels. Inlet performance was also observed for a range of inlet centerbody and engine settings.

The present study with the XB-70 airplane was directed toward evaluating inlet aerodynamic choking as a noise-suppression technique and toward determining the resultant inlet and engine performance. The XB-70 inlets, with their large size and Mach 3 design, are typical of future supersonic inlets and are characterized by sharp leading edges and variable geometry. Tests were made at several power settings ranging from 60 percent to 100 percent of full rated engine speed and at several throat areas with the XB-70 on a thrust stand. (A power setting of 87 percent was typically used during XB-70 landings.) The measurements were made at Edwards Air Force Base, Calif. The results of the tests are presented in terms of sound pressure levels, inlet pressure recovery, and net thrust for a range of engine speeds and inlet throat settings.

SYMBOLS

A_c	inlet capture area, per side, 5600 in.^{2} (3.62 m^2)
A_{th}	inlet cross-sectional area at the throat, in.^{2} (m^2)
$\frac{A_{th}}{A_c}$	inlet contraction ratio
B	number of blades on first compressor stage
D	flow distortion, $\frac{(p_{t_{max}} - p_{t_{min}})}{\bar{p}_t}$
F_N	thrust as indicated by direct measurement of force on thrust stand, lb (N)
f_c	compressor fundamental frequency
p	static pressure, lb/in.^{2} (N/m^2)
p_t	total pressure, lb/in.^{2} (N/m^2)
$\frac{p_{t_2}}{p_{t_o}}$	inlet total-pressure recovery, area-weighted average at the compressor face as compared with free-stream total pressure
R	compressor-face radius, in. (m)
r	radius from center of engine hub to total-pressure-probe tip, in. (m) (see fig. 13)

Subscripts:

o	free-stream (ambient) conditions
2	diffuser outlet station, engine compressor face (station 2028 in. (51.511 m))
duct	based on all compressor-face total pressures for the left duct
engine	based on individual engine averaged conditions
max	maximum
min	minimum

Superscript:

-	arithmetic averaged conditions

ABBREVIATIONS

dB	decibels, ref. 0.00002 N/m^2
mil	military power setting, 100-percent rpm
rpm	revolutions per minute

TEST AIRCRAFT

The XB-70 (fig. 1) is a large, supersonic aircraft in the 500,000-pound (227,000-kilogram) class, powered by six YJ93-GE-3 afterburning turbojet engines

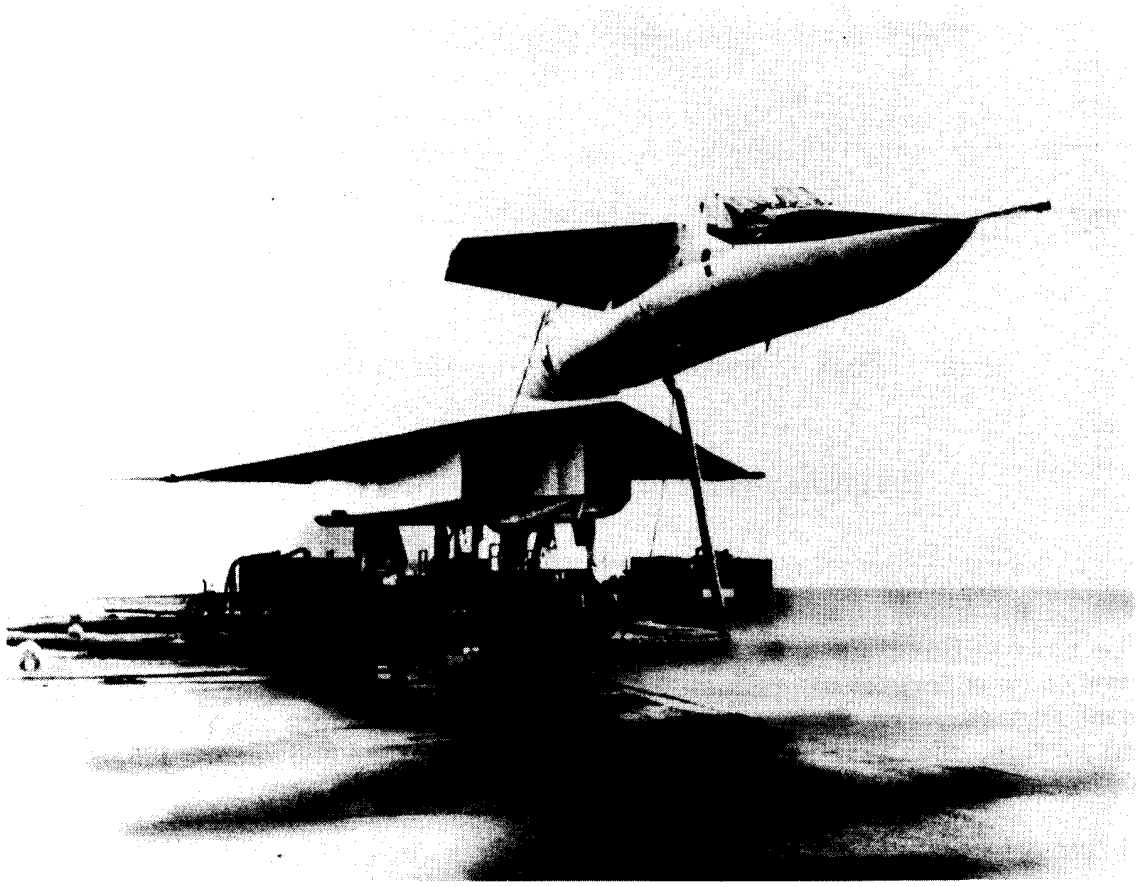

Figure 1.– Front view of the XB-70 airplane on the thrust stand.

installed side by side. Each engine is capable of thrust in the 30,000-pound (133,000-newton) range. The two-dimensional inlets, designed for Mach 3 operation, use movable throat ramps which vary the throat width from a nominal 48 inches (1.219 meters) to a nominal 22 inches (0.559 meter) and variable bypass doors near the exit which optimize propulsion-system performance through a wide range of flight conditions. Each inlet supplies air to three engines and is approximately 69 feet (21 meters) long with a projected frontal area of about 39 feet^2 (3.62 meters^2). Figure 2 is a schematic drawing of the left inlet. Detailed dimensions of the XB-70 airplane are included in reference 7.

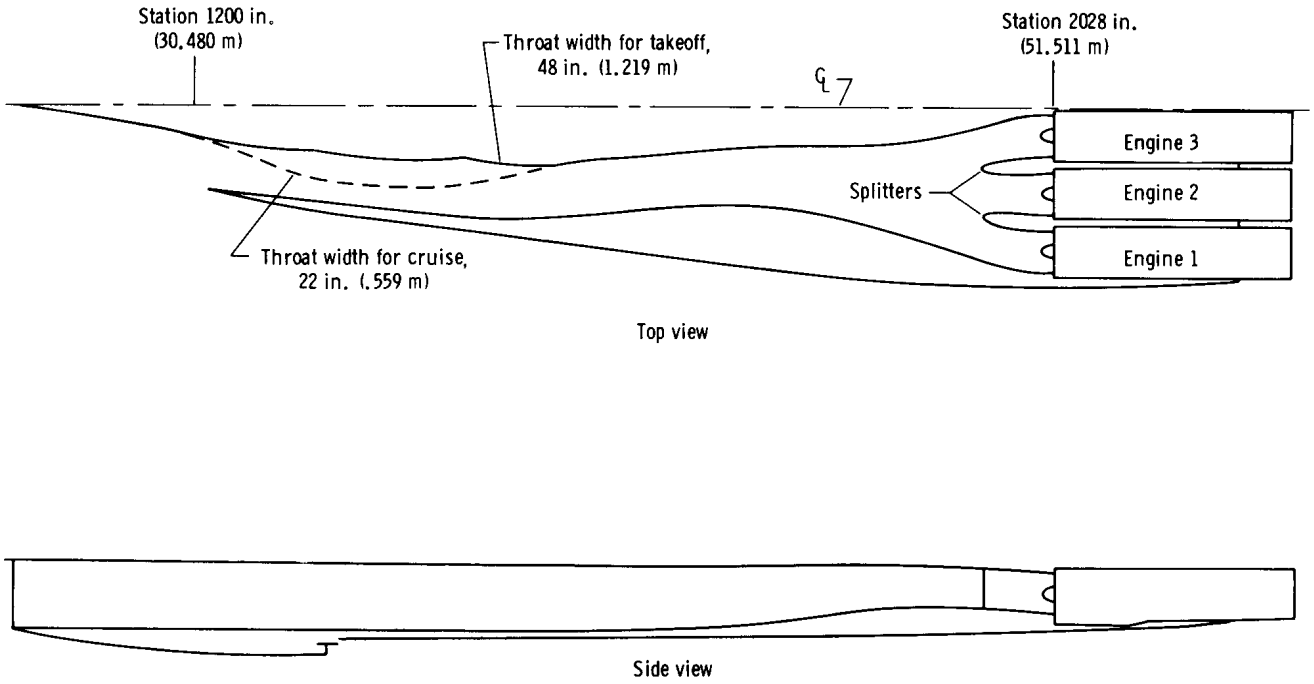

Figure 2.– Schematic drawing of the XB-70 left inlet.

INSTRUMENTATION AND DATA REDUCTION

Thrust Stand

The aircraft thrust-measurement facility, or thrust stand, used in this study is contained in an underground, reinforced-concrete structure with four separate loading platforms (fig. 3). The platforms and aircraft attachment points are flush with the run pad surface. Each platform is instrumented to measure and record 125,000 pounds (556,027 newtons) of thrust.

Thrust data are presented on four recorders, one for each platform. The thrust-measurement facility is capable of measuring within 0.25 percent of full scale.

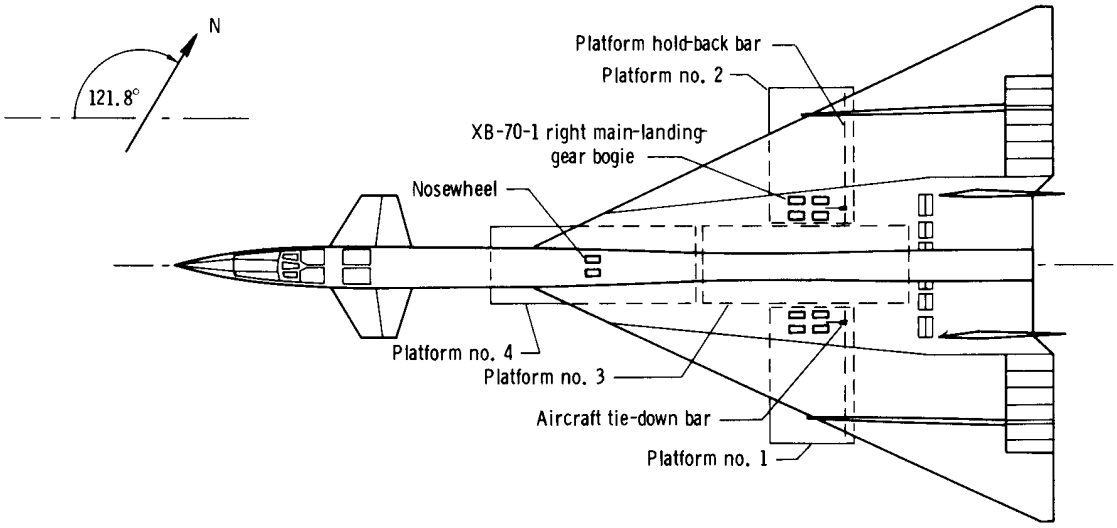

Figure 3.– XB-70 on the Edwards Air Force Base thrust stand (top view).

Inlet

Figure 4 shows the locations of the principal inlet pressure instrumentation used during this study. Table I lists the location, accuracy, and range of all inlet pressure

TABLE I

XB-70 INLET PRESSURE INSTRUMENTATION

(a) Duct static pressures.

Fuselage station, in. (m)	Parameter	Accuracy, percent full range	Transducer range, psid (N/m^2)
1222 (31.039)	Unstart signal static pressure	0.7	±15 (±103,400)
*1301 (33.045)	Outboard wall static pressure	2.5	±6 (±41,400)
*1334 (33.884)	Outboard wall static pressure	2.5	±15 (±103,400)
*1325 (33.655)	Outboard wall static pressure	2.5	±15 (±103,400)
*1337 (33.960)	Outboard wall static pressure	2.5	±6 (±41,400)
*1343 (34.112)	Outboard wall static pressure	2.5	±6 (±41,400)
*1349 (34.265)	Outboard wall static pressure	2.5	±6 (±41,400)
*1357 (34.468)	Outboard wall static pressure	2.5	±6 (±41,400)
*1369 (34.773)	Outboard wall static pressure	2.5	±15 (±103,400)
*1373 (34.874)	Outboard wall static pressure	2.5	±6 (±41,400)
1420 (36.068)	Downstream shock signal pressure	1.5	±15 (±103,400)
1750 (44.450)	Duct inboard wall static pressure	2.5	±15 (±103,400)
1795 (45.593)	Duct inboard wall static pressure	2.5	±30 (±206,800)
1948 (49.479)	Duct overpressure limit static pressure	1.5	±20 (±137,900)

*Wall throat-shock sensor-strip transducer.

(b) Compressor-face probes.

Engine number	Parameter	Accuracy, percent full range	Transducer range, psid (N/m^2)
1	21 total-pressure probes (fig. 4)	1.5	±6 (±41,400)
2	21 total-pressure probes (fig. 4)	1.5	±6 (±41,400)
3	21 total-pressure probes (fig. 4)	1.5	±6 (±41,400)

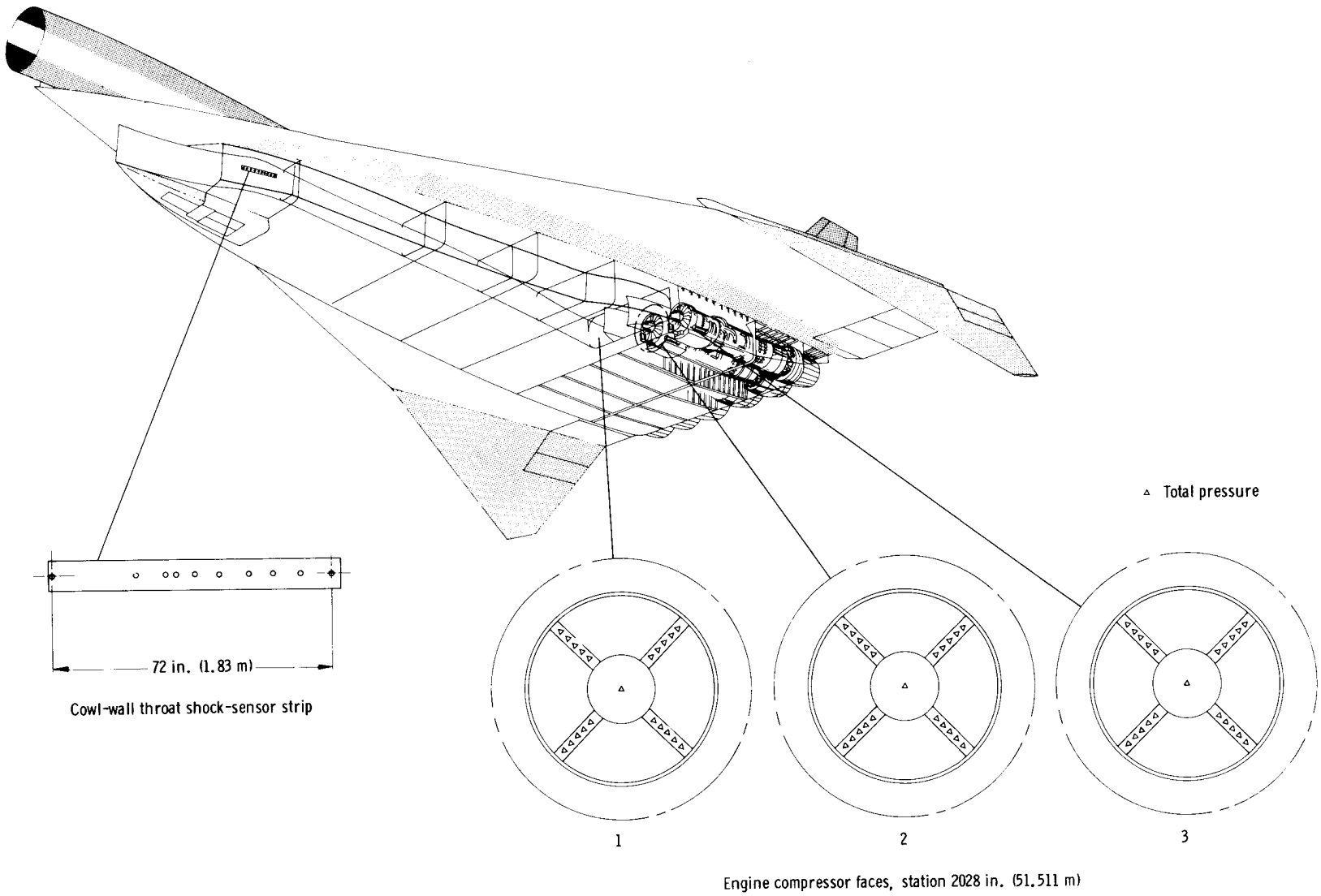

Figure 4.– Locations of XB-70 inlet instrumentation.

instrumentation. The instrumentation consisted of inlet-duct static-pressure sensors, a throat-ramp displacement indicator, and compressor-face total-pressure probes. Each engine compressor face had four symmetrically positioned total-pressure rakes with five total-pressure probes, each located at the center of equal cross-sectional areas. A total-pressure probe was also mounted at the center of each engine bullet nose or hub. The rakes installed on a typical YJ-93-3 engine are shown in figure 5.

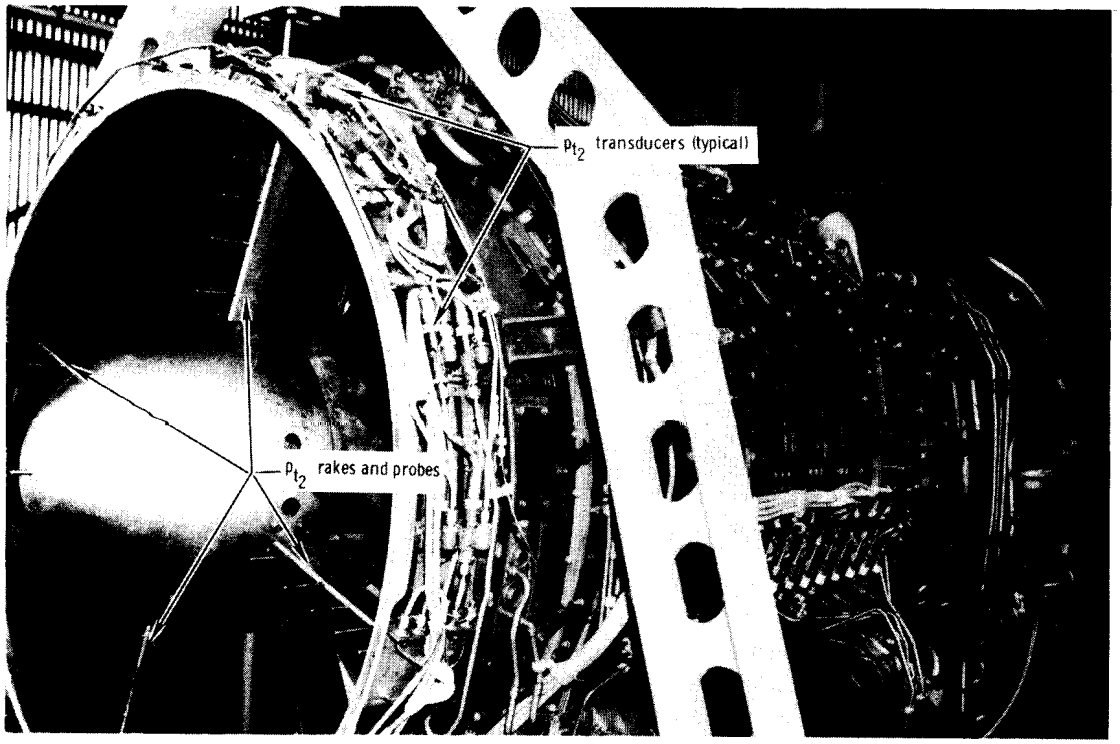

Figure 5.– Compressor-face instrumentation installation.

The outputs from the compressor-face total-pressure transducers and inlet static-pressure sensors were recorded on digital tape onboard the airplane. Calibrations and corrections were applied to the outputs of the tapes at the ground data-processing station. The data were then reduced on a digital computer to obtain total-pressure recovery, static-pressure distributions, and other calculated parameters presented in this report. The airplane and ground station data systems used in reducing the inlet and thrust-calculation data are described and discussed in references 8 to 10. The net accuracy of the pressure data was ±2.5 percent of full scale or better for the ranges shown in table I. The accuracy of the total-pressure recoveries was estimated to be better than 1 percent.

Acoustic

Instrumentation. – The microphone array used in the varied-throat-area and varied-engine-speed tests is shown in figure 6. These tests are described in detail in the Operational Procedures section. The array radius for the varied-throat-area tests was taken from the geometric center of the left-inlet opening. Microphones were placed on

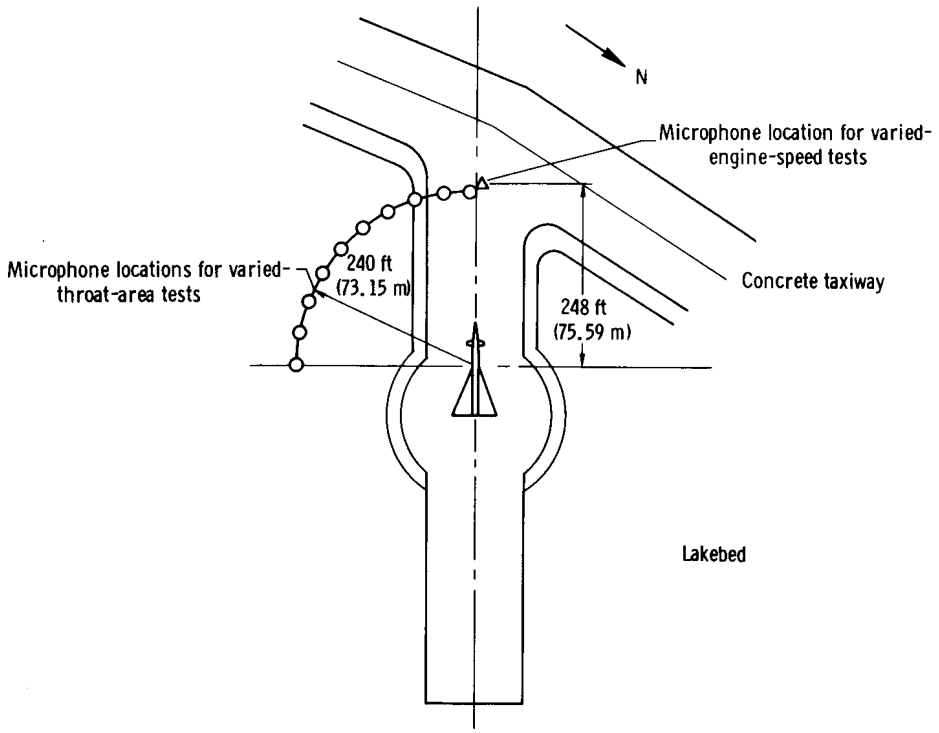

Figure 6.– Microphone array used in the varied-throat-area and varied-engine-speed tests.

adjustable poles at the height of the geometric center of the inlet opening. The microphones were positioned at heights from the ground of 4 feet (1.29 meters) at 0° to 10 feet (3.05 meters) at 90° from the airplane nose to account for the gently sloping terrain to the left of the thrust stand. The microphone used in the varied-engine-speed tests was placed on a pole centered ahead of the right inlet and at the height of the geometric center of the inlet opening.

A block diagram of one of the acoustic data-acquisition systems is shown in figure 7. The microphone formed the capacitive element of a tuned radio-frequency circuit which was connected to an oscillator-detector circuit by means of a low-impedance cable. The detected signal was then amplified and recorded on an instrumentation type of magnetic-tape recorder. An acoustic calibration was applied before and after each day's test to each microphone system at four different levels to verify system linearity. In addition, an electrostatic calibration was applied to each microphone system before the beginning of the tests to determine the frequency response.

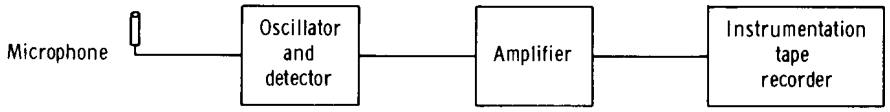

Figure 7.– Block diagram of one of the acoustic data-acquisition systems.

Data reduction. – A block diagram of the octave-band data-reduction system is shown in figure 8(a). The data were played back by using an instrumentation type of magnetic-tape recorder and were passed through the octave-band analyzer. The data were then linearly rectified, averaged, logarithmically amplified, and recorded on the strip-chart recorder.

The acoustic and electrostatic calibrations were processed through the primary data-reduction system so that corrections, as a function of frequency, could be determined for the entire data-acquisition and reduction system. The resultant corrections were then applied to the data to compensate for the nonlinearities induced by the acquisition and reduction systems. Background noise was also subtracted from the data.

There is an uncertainty in the acoustic octave-band data as a result of uncertainties in the calibration, data acquisition, data reduction, and human reading of the oscillograph recorder. The total root-mean-square error, based on estimates of these errors, is about ±1 decibel.

A block diagram of the narrow-band analysis system is presented in figure 8(b). The magnetic tapes, containing the data of interest, were cut and formed into loops. The data were recovered by using the loop tape recorder and subsequently analyzed by using a 10-hertz bandwidth filter over the range of 50 hertz to 300 hertz, a 50-hertz bandwidth filter over the range of 300 hertz to 1000 hertz, and a 100-hertz filter over the range of 1000 hertz to 10,000 hertz.

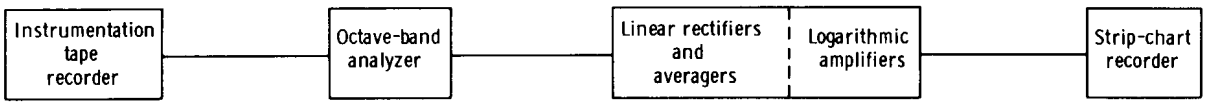

(a) Octave-band system.

(b) Narrow-band system.

Figure 8. – Block diagrams of the octave-band and narrow-band data-reduction systems.

The narrow-band acoustic analysis was done only for comparison purposes; thus, no absolute error was estimated and no background-noise corrections were made, inasmuch as only frequencies below 500 hertz would be affected. The averaging time was such that the 90-percent statistical confidence interval was ±1/2 decibel.

TEST DESCRIPTION

Operational Procedures

The original intent of the tests was to gradually cause the inlet flow to choke by making successive small reductions in the left-inlet throat area. The engines were set at full military speed (100-percent rpm), and the throat was then closed in steps to a point slightly beyond choked. After the first choking, the engine speed was reduced to 87 percent of full speed. The reduction in speed and engine airflow unchoked the inlet. The inlet throat area was then again reduced until another choked-flow condition was reached.

The progression of these varied-throat-area tests was closely monitored by means of telemetered data. The key data telemetered were the static pressures measured in the inlet throat region and the pressure ratio across part of the inlet duct wall. The throat pressures indicated the choking, and the pressure across the wall indicated the level of duct pressure load which was related to a structural and, therefore, a safety limit.

After the data from the varied-throat-area tests were reduced, it became apparent that additional tests were required. Consequently, tests were conducted in which the inlet throat area was held at a fixed, full-open setting and engine speeds were increased in steps from 60 percent to the final 87 percent of full rpm. Since these varied-engine-speed tests were conducted after an XB-70 flight, only acoustic data were obtained because engine shutdown procedure required that the data be taken from the right-side inlet, which was not adequately instrumented to obtain performance data.

The engine and inlet throat settings used in the tests are presented in table II, and

TABLE II

TEST SCHEDULE OF INLET AND ENGINE SETTINGS

Throat				Contraction ratio, A_{th}/A_c	Engine power settings, percent rpm	
Width,		Area,				
in.	m	in.^{2}	m^2		Left inlet	Right inlet
Varied-throat-area tests (left inlet)						
47.6	1.209	3113	2.008	0.556	100 (military)	--------
39.2	0.996	2564	1.654	.457	100 (military)	--------
37.3	.947	2439	1.574	.435	100 (military)	--------
35.1	.892	2296	1.481	.409	100 (military)	--------
33.2	.843	2171	1.400	.387	100 (military)	--------
31.7	.805	2073	1.337	.370	100 (military)	--------
31.7	.805	2073	1.337	.370	87	--------
29.6	.752	1936	1.249	.345	87	--------
27.8	.706	1818	1.173	.324	87	--------
25.7	.653	1680	1.084	.300	87	--------
24.0	.610	1570	1.013	.279	87	--------
23.6	.599	1543	.995	.276	87	--------
Fixed-throat-area tests (right inlet)						
48.0	1.219	3139	2.025	.560	----------	60
48.0	1.219	3139	2.025	.560	----------	70
48.0	1.219	3139	2.025	.560	----------	80
48.0	1.219	3139	2.025	.560	----------	87

the cross-sectional-area distribution of the inlet for selected throat settings is shown in figure 9.

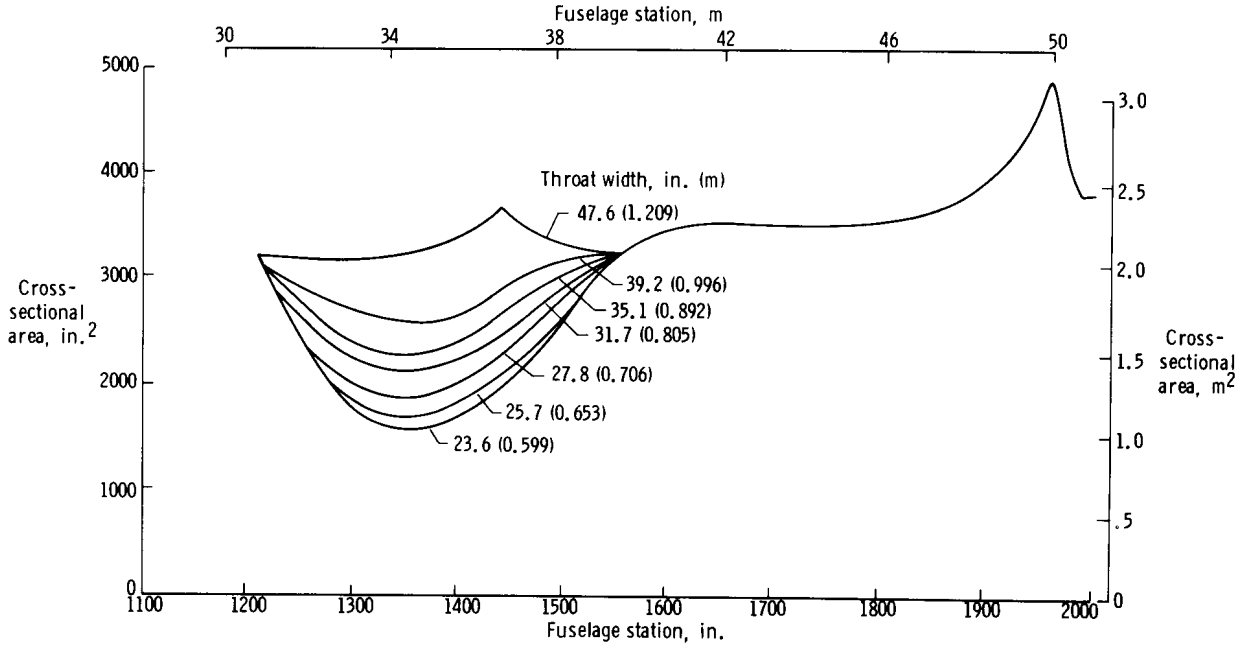

Figure 9.– Duct cross-sectional area distribution for several throat widths obtained during the varied-throat-area tests.

Environmental Conditions

The terrain surrounding the thrust stand in which the variable-throat-area tests were conducted was clear of obstructions, with a concrete taxiway directly in front of the airplane (fig. 6). Ground support equipment, which was near the aircraft during all the tests, contributed significant noise at engine power settings of 87-percent rpm and below in the frequencies below 500 hertz. Although the airplane was not on the thrust stand for the varied-engine-speed tests, the environment was essentially the same as for the varied-throat-area tests.

The weather conditions for each test are summarized in the following table:

Test	Temperature, °F (°C)	Relative humidity, percent	Atmospheric pressure, lb/ft^2 (N/m^2)	Wind velocity, knots (m/sec)	Wind direction from aircraft heading, deg
Varied throat area	50 (10.0)	70	1954 (93,561)	Calm	Calm
Varied engine speed	51 (10.5)	17	1957 (93,707)	14 (7.2)	0

Even though the wind velocity was 14 knots (7.2 meters/second) in the varied-engine-speed tests and there was background noise in both tests, neither of these conditions is believed to have affected the acoustic data at frequencies above 500 hertz.

RESULTS AND DISCUSSION

Propulsion-System Performance

The propulsion-system performance was measured and recorded during the varied-throat-area tests. The performance, in terms of inlet distortion, total-pressure recovery, and measured net thrust, was related to the simultaneous external acoustic data. Propulsion-system data were not recorded during the fixed-throat, varied-engine-speed tests, so propulsion performance is shown only for the varied-throat-area tests.

The initial tests resulted in a choked-flow region in the duct as the throat area was reduced. The choking was indicated as shown in figures 10(a) and 10(b) by the pressure ratio $\frac{p}{p_{t_o}}$, which decreased below the theoretical value for choked flow in the inlet throat region. The increase in pressure ratio in the region near the cowl lip with

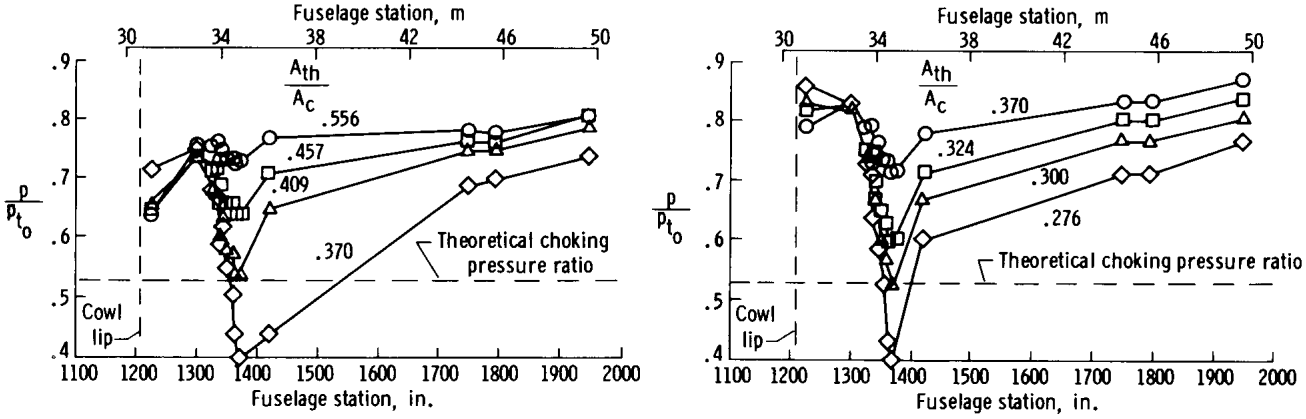

(a) Military power (100 percent rpm). *(b) 87-percent rpm.*

Figure 10.– Duct static-pressure-ratio distribution versus fuselage station and contraction ratio for selected varied-throat-area tests.

decreasing contraction ratio results from the lower flow velocities caused by the reduction in airflow. The decrease in pressure ratio in the throat region with decreasing contraction ratio is due to the increasing flow velocity in that region. The lower static pressures near the cowl lip for the military power setting suggest a possible flow separation (or tripping) near the sharp leading edge of the cowl. This is evident in the photograph of figure 11 in which the flow separation can be seen near the lower leading edge of the inlet opening. The white area was observed when the relatively moist air was tripped by the sharp edge, resulting in a condensate forming in the flow. When this photograph was taken, the right-side engines were not operating.

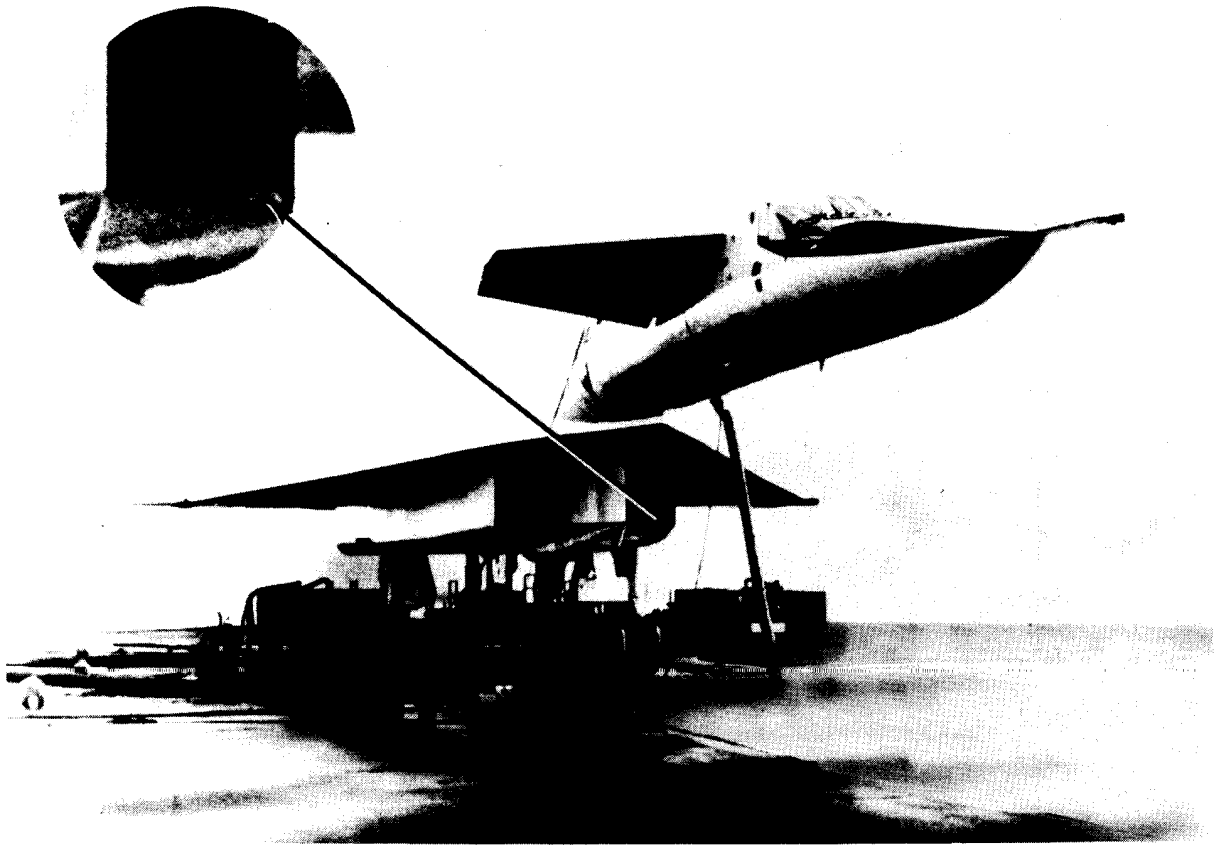

Figure 11.– Illustration of sharp-lip flow separation.

The propulsion-system performance during the varied-throat-area tests is presented in figures 12(a) and 12(b) in terms of area-weighted (average over equal compressor-face areas) total-pressure recovery, distortion, and directly measured thrust plotted against inlet contraction ratio. The contraction ratios corresponding to inlet choking were obtained from figure 10. The total-pressure recovery decreases from 0.86 to 0.77 (10 percent) for military power and from 0.89 to 0.78 (12 percent) for 87-percent rpm as the inlet contraction ratio decreases over the test range. As a result of the sharp lips on the inlet, significant total-pressure-recovery loss occurs before the inlet is theoretically choked. Total-pressure recovery decreases as choking is approached, with the lowest pressure recovery at the minimum throat condition for each engine speed.

Figure 12(a) also shows a theoretical estimate (ref. 11) of the total-pressure recovery for military power. At choked throat conditions $\left(\frac{A_{th}}{A_c} = 0.4\right)$ the total-pressure-recovery estimate is 0.92. In the theoretical estimate, lip losses were estimated by using a momentum balance from ambient conditions to the lip station. It was assumed that no loss occurred between the lip station and the inlet throat and that losses between the inlet throat and engine station were proportional to the throat dynamic pressure. The large differences between the estimated and measured total-pressure recovery indicate large viscous and separation losses in the duct regions where rapid area changes occur (fig. 9).

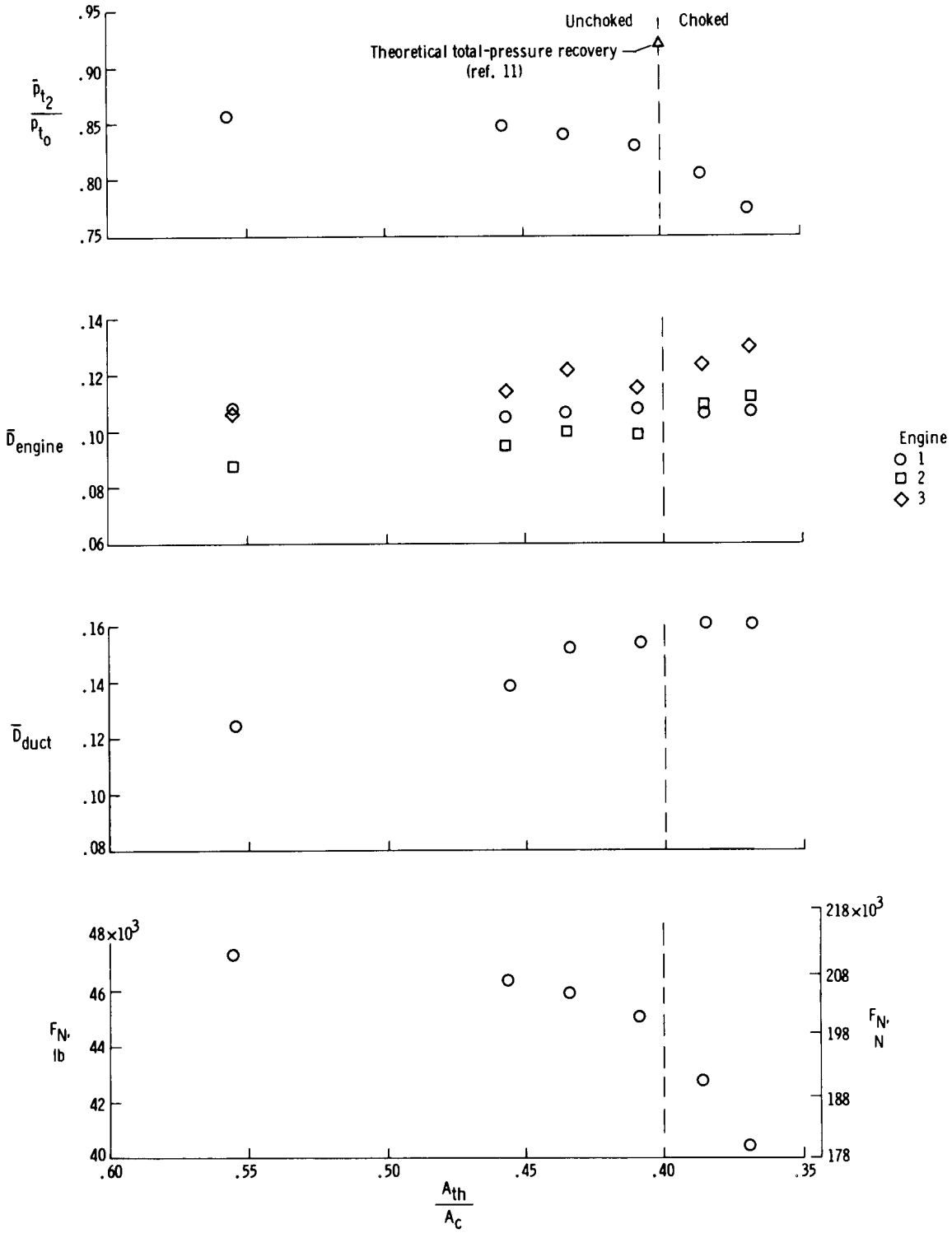

(a) Military power.

Figure 12.– Propulsion-system performance versus inlet contraction ratio at two engine speeds for the varied-throat-area tests.

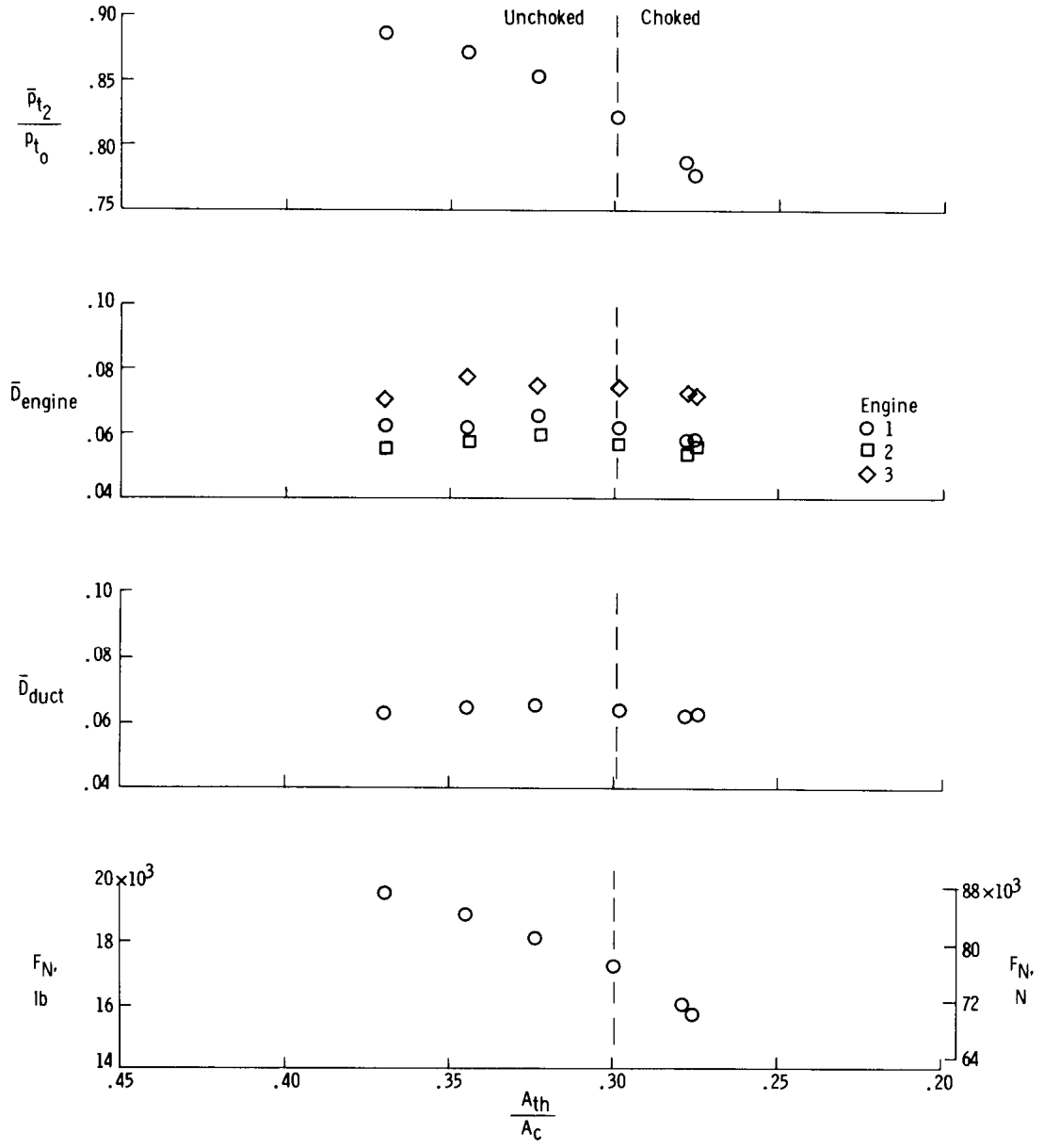

(b) 87-percent rpm.

Figure 12.– Concluded.

Distortion was almost constant for both power settings as choking was approached. This indicates that the turbulent flow must have mixed well in the long duct before the flow reached the compressor faces. The thrust levels, however, reflect the lower total-pressure recovery and reduced mass flow associated with choking and decrease 14 percent for the military power range of throat settings and 18 percent for the tests at 87-percent rpm.

Figures 13(a) and 13(b) present the complete total-pressure distribution for each engine. The distributions and calculated averages are shown only for the extreme (unchoked and choked) conditions of the tests. The data show a more uniform

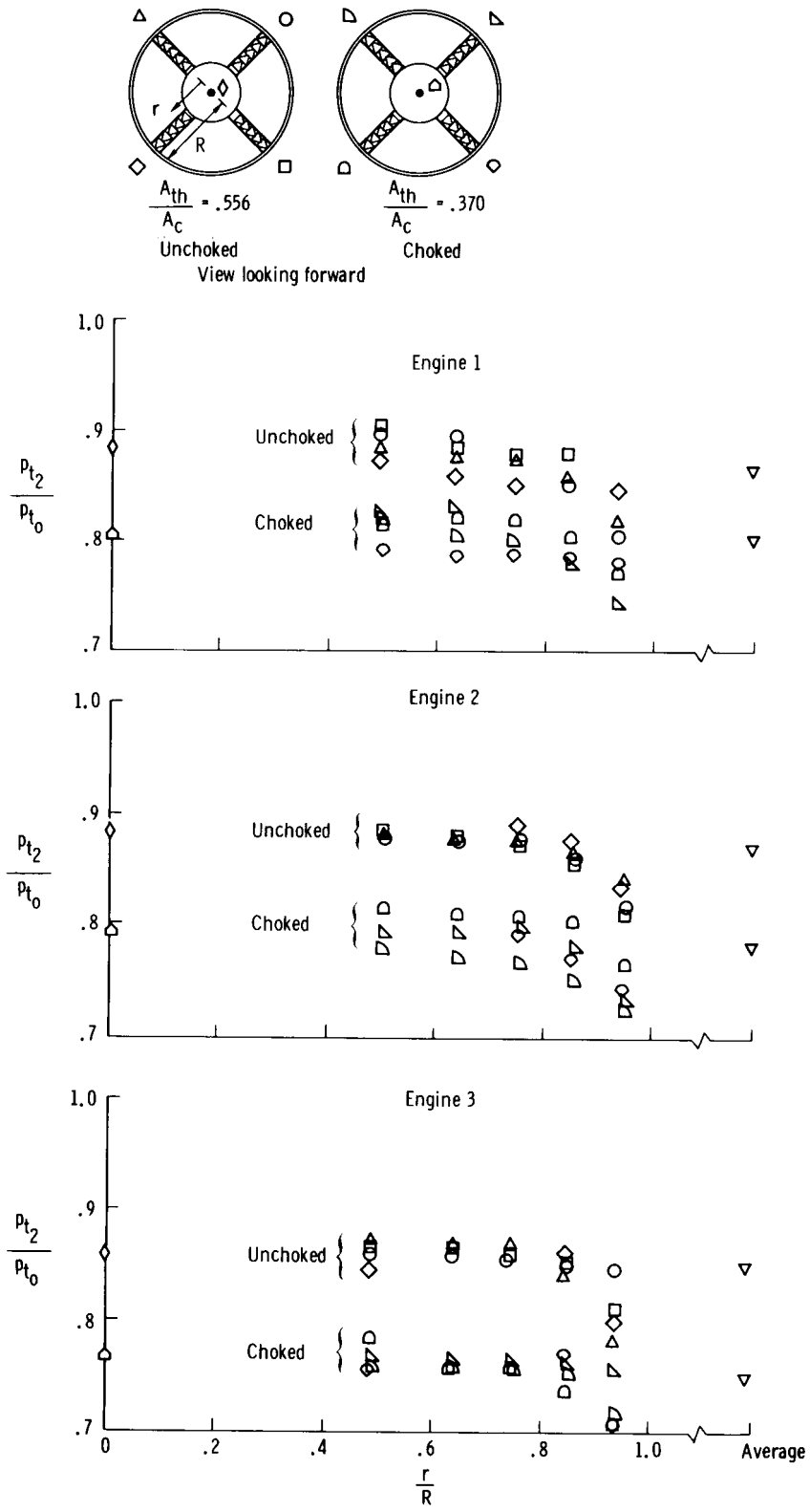

(a) Military power.

Figure 13.– Total-pressure-recovery distributions at choked and unchoked throat settings for two engine speeds.

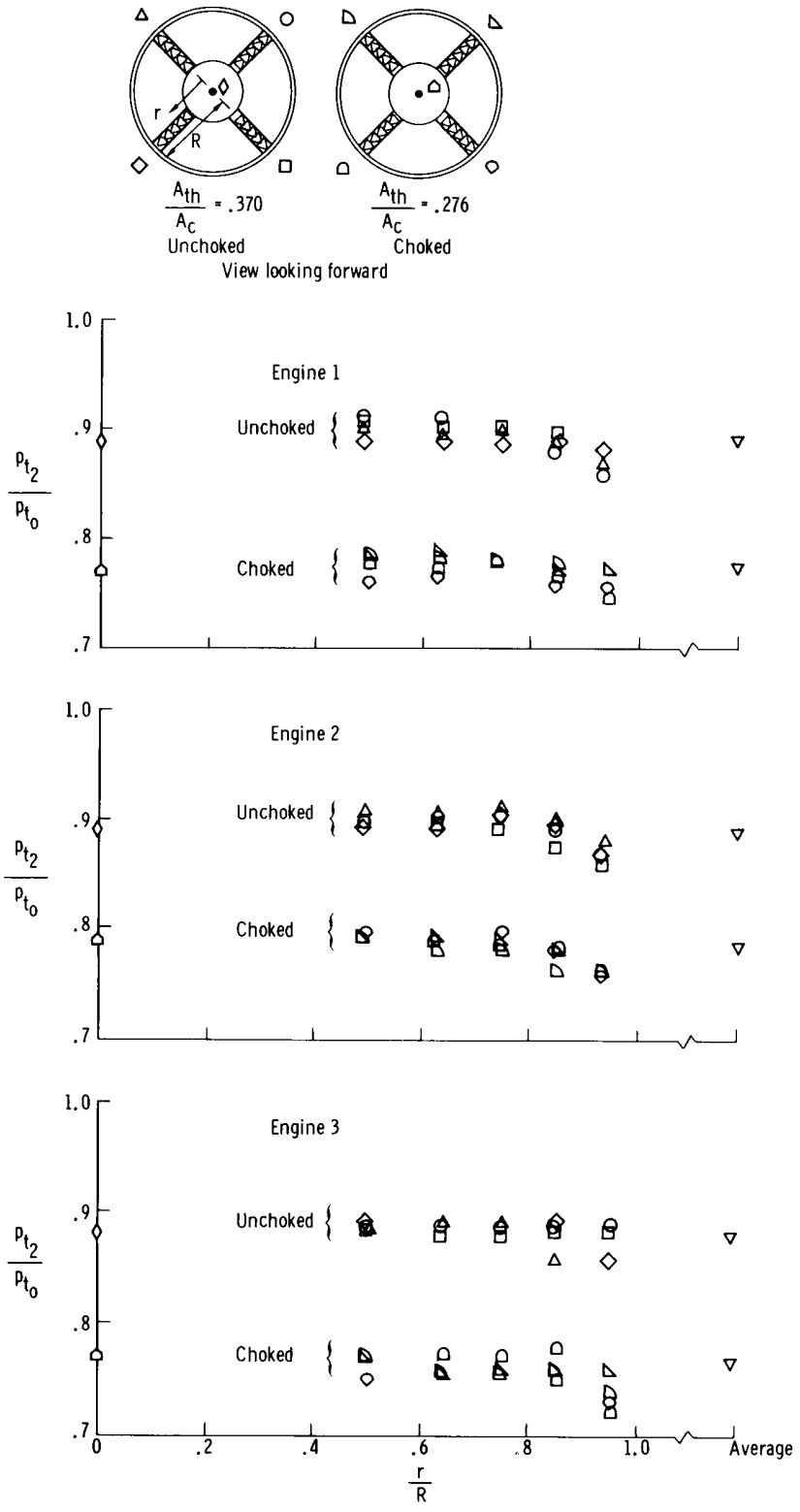

(b) 87-percent rpm.

Figure 13.– Concluded.

distribution for 87-percent rpm than for military power for both the unchoked and choked conditions. For both power settings and all engines, the lowest values of total-pressure recovery occur near the maximum radius of the engine. The loss in average total-pressure recovery due to choking is greater for 87-percent rpm than for military power.

Acoustic Results

Acoustic data acquired during the varied-throat-area tests are presented in the form of sound-pressure-level spectra and contours. Only the noise spectra measured at 0° and a 240-foot (73.15-meter) radius are presented because the spectra were essentially the same for all positions. The octave-band spectra of the noise measured by the microphone positioned at 0° and a 240-foot (73.15-meter) radius are presented in figure 14. Spectra are shown for the unchoked and choked conditions of the left inlet at military power and 87-percent rpm. It should be noted that the shapes of the spectra are similar to those of the exhaust-noise spectra of the XB-70 (ref. 12). The compressor fundamental frequencies expected to show as peaks in the noise spectra were calculated to be between 2000 hertz and 4000 hertz by using the formula $f_c = \frac{(B)\ (rpm)}{60}$. However, the octave-band spectra do not exhibit a peak in the 2000-hertz or 4000-hertz

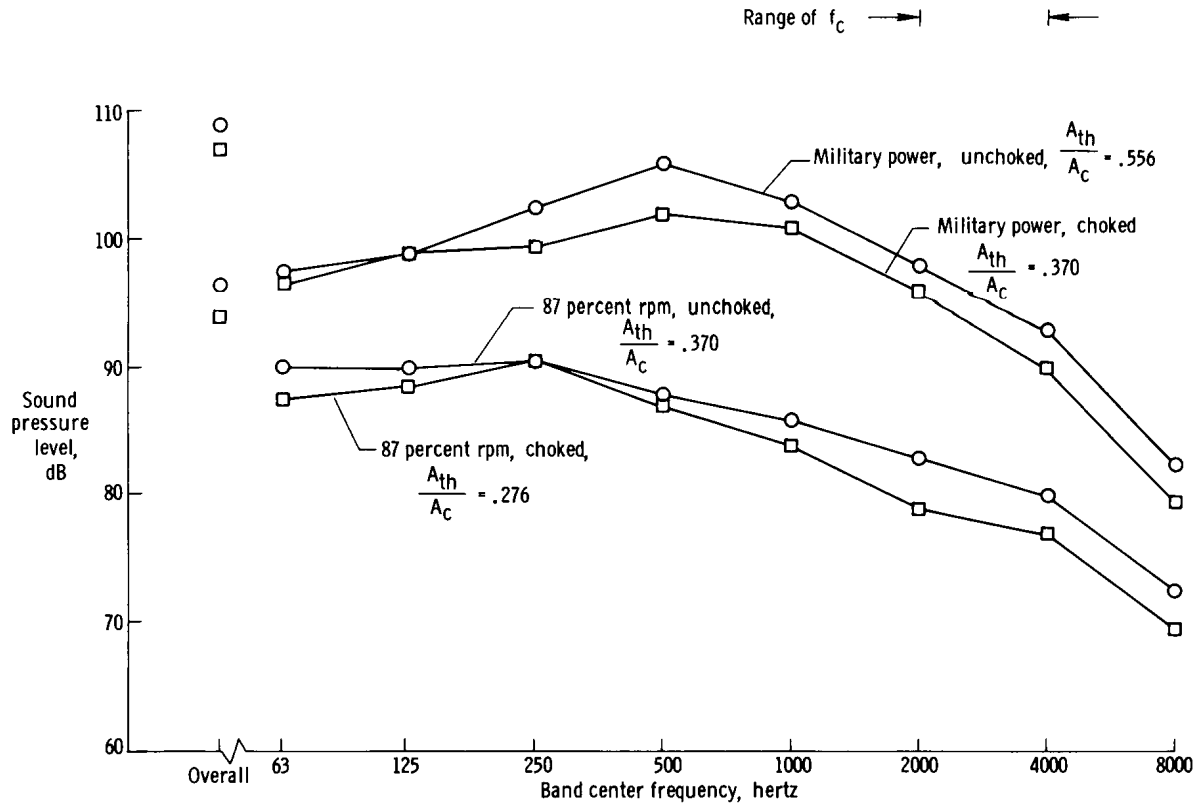

Figure 14.– Octave-band noise spectra at 0° and 240 feet (73.15 meters) from the left inlet for unchoked and choked conditions at two engine speeds.

bands in either the unchoked or choked conditions, which indicated that there were no discrete compressor frequencies. Consequently, a narrow-band analysis of the same data was made, with the results shown in figure 15. This analysis confirmed that there were no discrete compressor frequencies in the range of 2000 hertz to 4000 hertz radiated from the inlet under these test conditions.

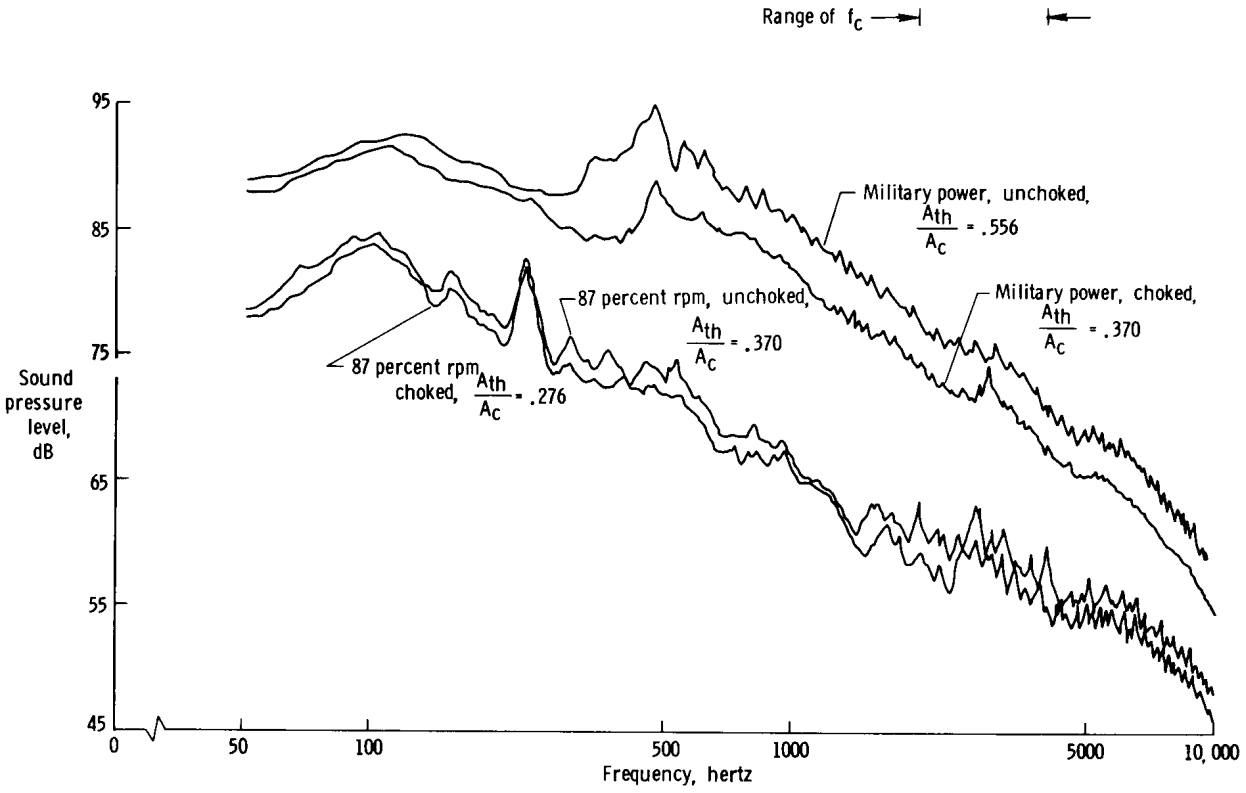

Figure 15.– Narrow-band noise spectra at 0^o and 240 feet (73.15 meters) from the left inlet for unchoked and choked conditions at two engine speeds.

Sound-level contours measured by the quarter-circle of microphones centered on the left inlet are presented in figure 16 for two engine power settings with the inlet unchoked and choked. At the military power setting, the contours showed a 2-decibel to 5-decibel decrease in overall sound pressure level when the inlet was choked; whereas, for 87-percent rpm, there was a 1-decibel to 3-decibel difference in overall sound pressure level between the unchoked and choked inlet conditions. These reductions in sound level probably resulted from corresponding reductions in thrust, as the inlet was choked, of 14 percent for military power and 18 percent for 87-percent rpm, as shown in figure 12. As noted previously, the reduced thrust is a result of the reduced mass flow through the engines caused by choking the inlet. The reduced mass flow reduces the jet noise, which also contributes to the noise measured in the forward quadrant.

As previously discussed, the absence of peaks in sound pressure level at the calculated compressor fundamental frequencies in the first tests suggested that these

peaks had already been attenuated at the test engine power settings. This indicated a need for more data at lower engine power settings; consequently, limited variable-engine-speed tests were conducted at a later date, using only the right-side inlet at the maximum throat opening.

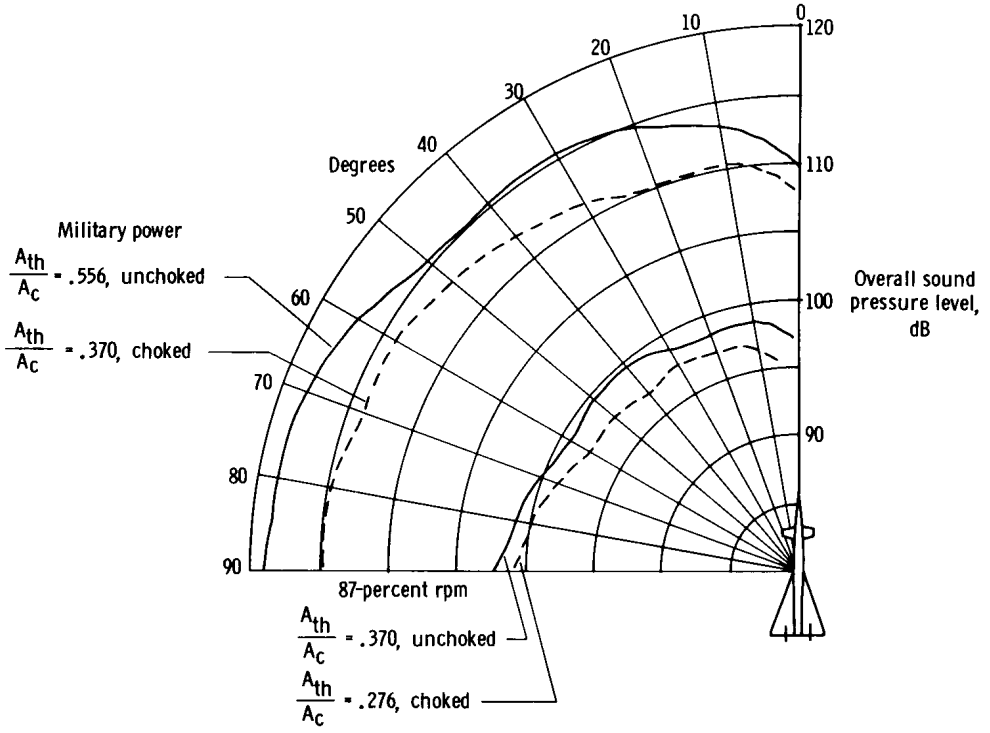

Figure 16.– Overall sound-pressure-level contours for the left inlet unchoked and choked at 87 percent rpm and military power settings.

The octave-band spectra of the noise radiated from the right inlet, measured at 0° from the inlet on a 248-foot (75.59-meter) radius for various power settings, are presented in figure 17. It should be noted that the compressor fundamental frequency shifts with changing rpm and that for 60-, 70-, 80-, and 87-percent rpm the calculated fundamental frequencies are 2457, 2867, 3265, and 3564 hertz, respectively.

In figure 17 the definite peak in the 2000-hertz octave band with the engines at 60-percent rpm indicates the presence of compressor-generated noise. As the engine speed was increased, the sound pressure level in the 2000-hertz octave band decreased because the compressor fundamental frequency shifted outside the 2000-hertz octave-band limits. Correspondingly, it would be expected that the sound pressure level of the 4000-hertz octave band would increase as the compressor fundamental frequency shifted into the 4000-hertz octave-band limits. However, although the sound pressure level of the 4000-hertz octave band increased for 70- and 80-percent rpm power settings, it then decreased as the speed was increased to 87 percent. The decrease in sound pressure level of the 4000-hertz octave band with increasing speed (above 80 percent) indicates attenuation of the compressor-generated noise.

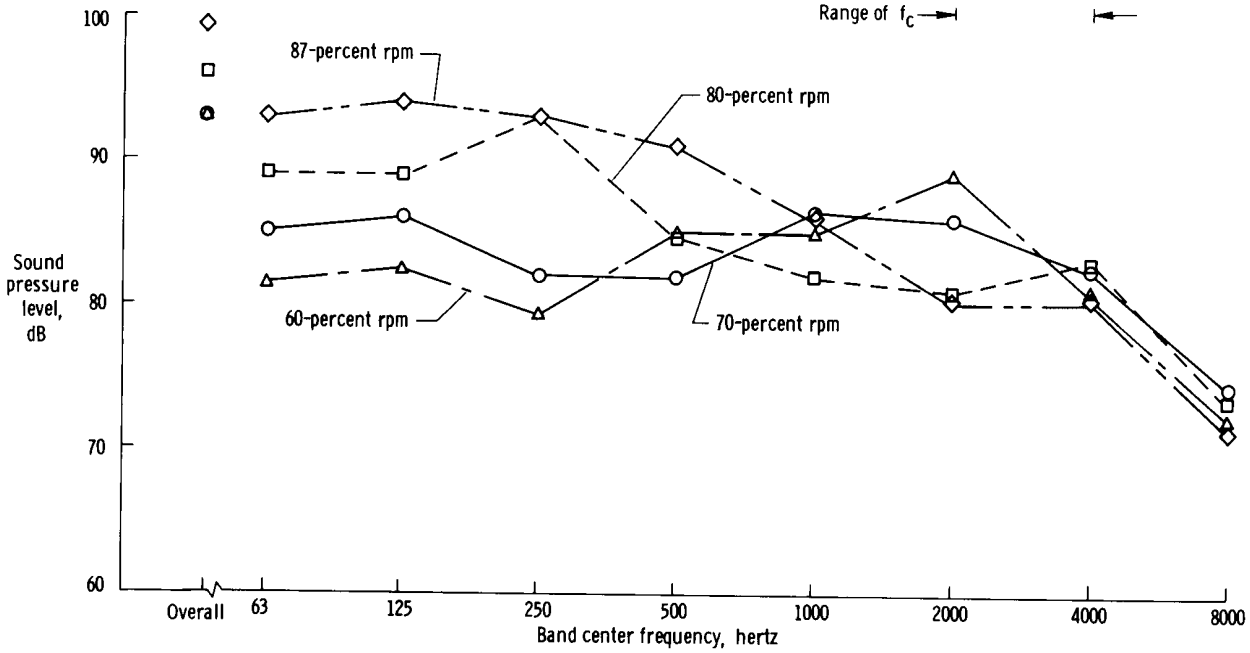

Figure 17.– Octave-band noise spectra at 0^o and 248 feet (75.59 meters) from the right inlet with engines at various engine speeds and throat at maximum opening. $A_{th}/A_c = 0.560$.

To resolve the specific frequencies, the same data were analyzed by using the narrow-band analyzer. The results are presented in figures 18(a) to 18(d). The peak sound pressure level at the compressor fundamental frequency is prominent for a power setting of 60-percent rpm but, by the time the engines are at 87-percent rpm, the peak has progressively broadened out and has decreased by approximately 10 decibels. Also, at 87-percent rpm the levels of all frequencies above 4000 hertz decreased 5 decibels to 7 decibels, compared with the levels at 60-percent rpm. Thus, it appears that the compressor noise was attenuated at 87-percent rpm with the throat at its maximum opening. The pressure measurements at the inlet wall that were presented in figure 10 for the previous tests indicate that the throat would be unchoked at its maximum opening for 87-percent rpm.

An additional observation can be made by comparing the data of figure 18(d) (87-percent rpm, $\frac{A_{th}}{A_c} = 0.560$) with those of figure 15 (87-percent rpm, $\frac{A_{th}}{A_c} = 0.370$). The absence of any peak in figure 15 at the blade-passing frequency indicates that decreasing $\frac{A_{th}}{A_c}$ for fixed engine speed also results in attenuation of the compressor noise. In each instance (fixed area ratio, increasing engine speed; and fixed engine speed, decreasing area ratio) the adjustment is from an unchoked toward a choked condition.

Apparently, little noise reduction was experienced in the varied-throat-area tests because the compressor noise was already attenuated to the noise level established by the jet exhaust at the beginning of the tests.

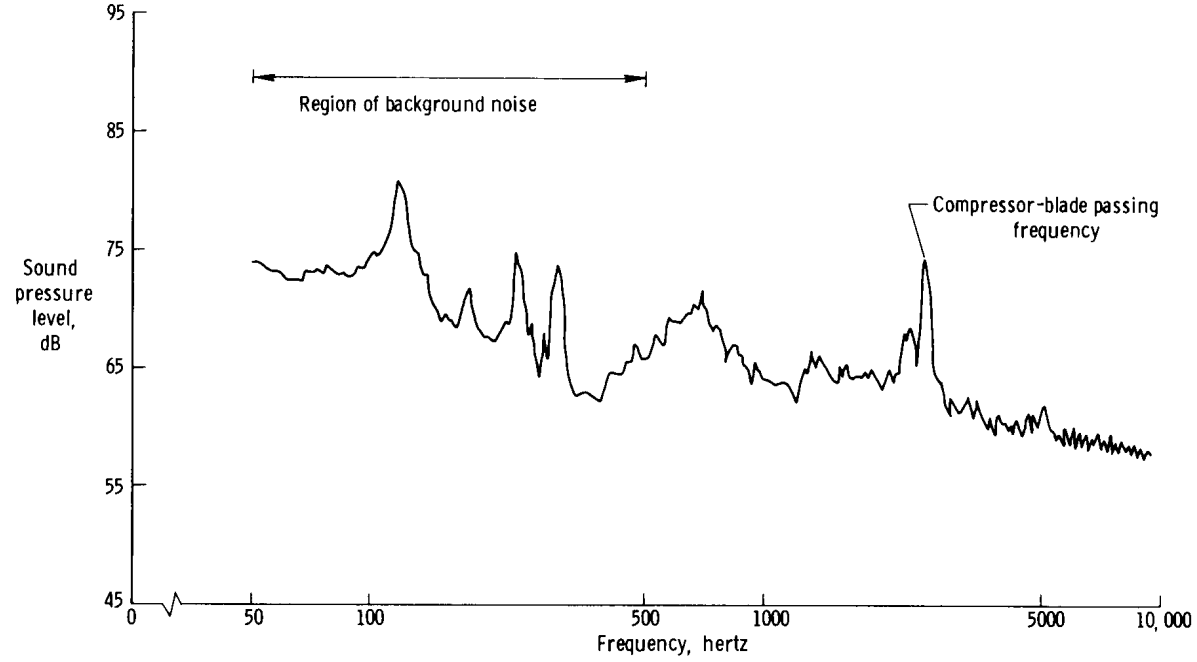

(a) 60-percent rpm.

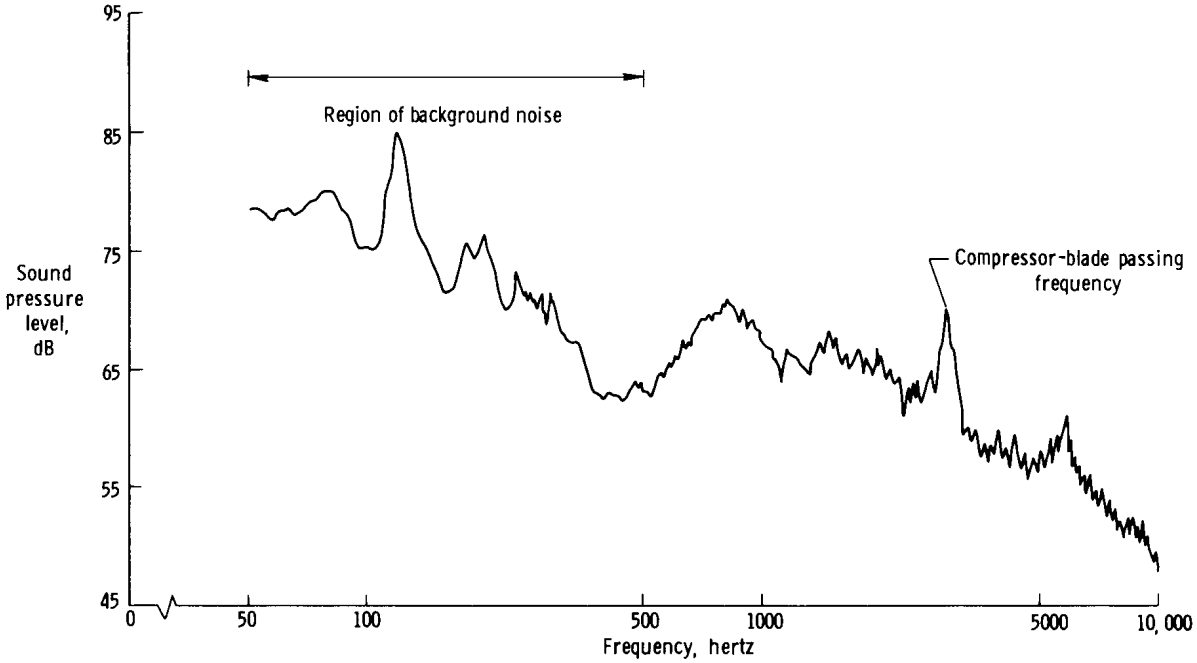

(b) 70-percent rpm.

Figure 18.– Noise spectra at 0^{o} and 248 feet (75.59 meters) from the right inlet with throat at maximum opening for various engine speeds.

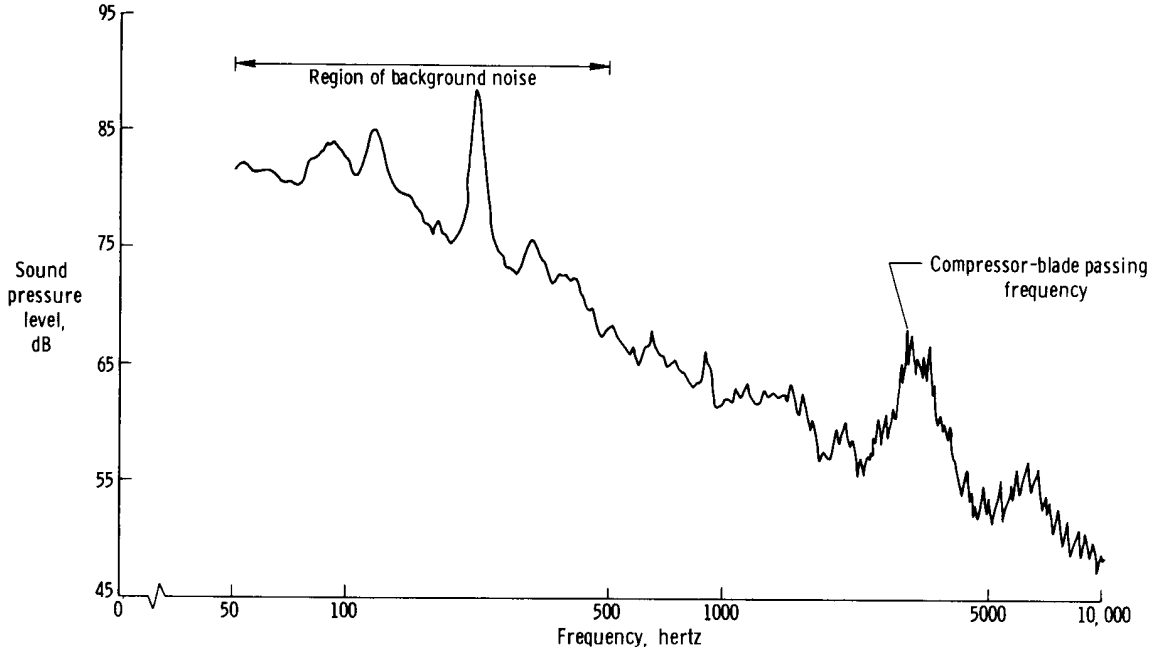

(c) 80-percent rpm.

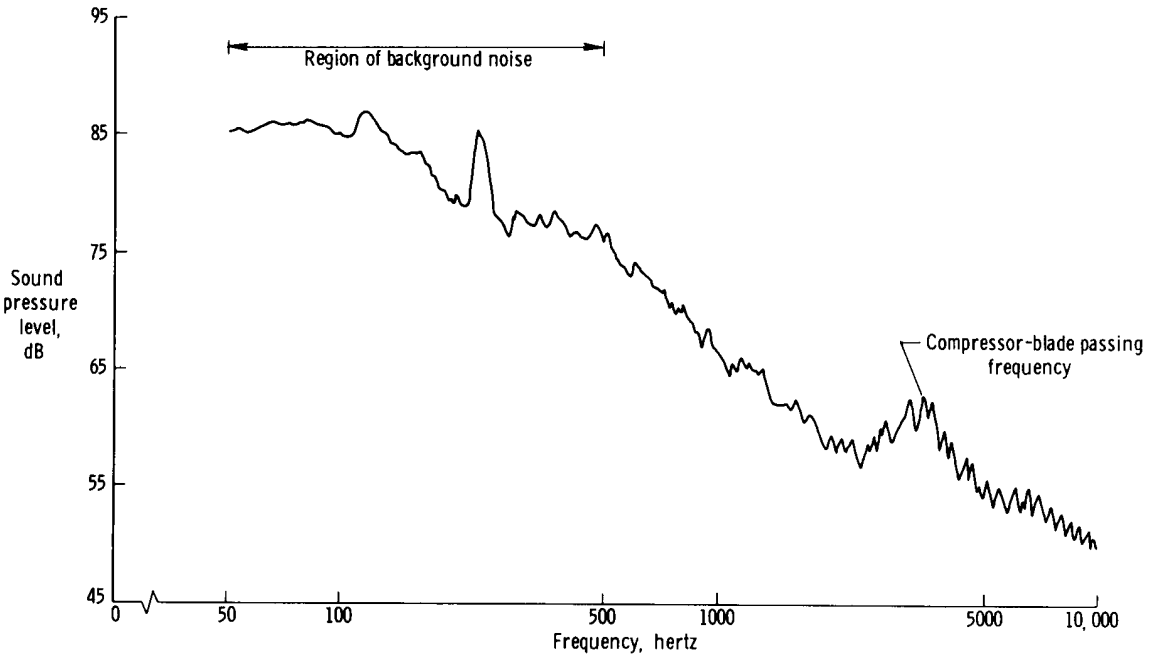

(d) 87-percent rpm.

Figure 18.– Concluded.

In the study of reference 3, noise-suppression tests were made on an inlet designed for subsonic flow by modifying the inlet with a variable cowl to achieve sonic flow. The compressor noise was also found to be attenuated to a noise level established by other sources prior to reaching sonic throat conditions. In reference 4 large reductions in compressor noise were observed just prior to sonic throat conditions when an inlet designed for subsonic operation was modified with a movable plug to achieve sonic flow. In tests on a supersonic inlet, the researchers of reference 6 indicate that some noise reduction occurred prior to choking but that their tests were not definitive enough to verify this.

CONCLUDING REMARKS

An investigation was conducted with the XB-70 airplane to determine the effect of choking an inlet on radiated compressor noise and propulsion-system performance.

It was found that inlet total-pressure recovery decreased significantly for a military power setting (100-percent rpm) and for a setting of 87-percent rpm as the inlet throat was choked. The values of choked recovery were lower than the more idealized predictions for a sharp-lipped inlet at zero speed. The disagreement suggests that more attention should be given to the duct internal-flow phenomena in future studies. Measured thrust decreased with the losses in total-pressure recovery.

The expected compressor-noise suppression was not experienced when inlet choking was induced by setting the throat at reduced openings for engine power settings of 87-percent rpm or military power. The noise suppression was not achieved because the compressor noise had already been reduced to the noise level established by the jet exhaust at the beginning of the varied-throat-area tests, although pressure measurements at the inlet wall did not indicate a choked condition.

The results of the varied-engine-speed, constant-throat-area tests indicated that the compressor noise was attenuated about 10 decibels when engine speed was advanced from 60-percent rpm to 87-percent rpm, even though the inlet was not choked. These results suggest that for an inlet of this type it may not be necessary to completely choke the inlet to achieve the desired noise suppression.

Flight Research Center,
National Aeronautics and Space Administration,
Edwards, Calif., November 26, 1969.

REFERENCES

1. Marsh, Alan J.; Elias, I.; Hoehne, J. C.; and Frasca, R. L.: A Study of Turbofan-Engine Compressor-Noise-Suppression Techniques. McDonnell Douglas Corp. (NASA CR-1056), 1968.

2. Lowson, M. V.: Reduction of Compressor Noise Radiation. J. Acoust. Soc. Am., vol. 43, no. 1, Jan. 1968, pp. 37-50.

3. Higgins, C. C.; Smith, J. N.; and Wise, W. H.: Sonic Throat Inlets. Progress of NASA Research Relating to Noise Alleviation of Large Subsonic Jet Aircraft, NASA SP-189, 1968, pp. 197-215.

4. Carmichael, R. F.; and Pelke, D. E.: In-Flight Noise Measurements Performed on the X-21A Laminar Flow Aircraft. NOR-64-81 (Contract AF33(600)-42052, DDC No. AD 439351) Northrop Corp., Norair Div., Apr. 1964.

5. Sobel, J. A. III; and Welliver, A. D.: Sonic Block Silencing for Axial and Screw-Type Compressors. NOISE Control, Sept./Oct. 1961, pp. 9-11.

6. Cawthorn, Jimmy M.; Morris, Garland, J.; and Hayes, Clyde: Measurement of Performance, Inlet Flow Characteristics, and Radiated Noise for a Turbojet Engine Having Choked Inlet Flow. NASA TN D-3929, 1967.

7. Kordes, Eldon E.; and Love, Betty J.: Preliminary Evaluation of XB-70 Airplane Encounters With High-Altitude Turbulence. NASA TN D-4209, 1967.

8. Ince, D. B.: Application Experience With the B-70 Flight Test Data System. Aerospace Instrumentation. Vol. 4 - Proceedings of the Fourth International Aerospace Symposium, College of Aeronautics, Cranfield, Eng., March 21-24, 1966, M. A. Perry, ed., Pergamon Press, Ltd., 1967, pp. 195-208.

9. Edwards, E. L.: A Data Processing Facility for the XB-70 Flight Test Program. Flight Test Instrumentation, AGARD Conf. Proc. No. 32, 1967, pp. 243-258.

10. Edwards, E. L.: An Airborne Data Acquisition System for Use in Flight Testing the XB-70 Airplane. Selected Instrumentation Application Papers From AGARD Flight Mechanics Panel - Twenty-Sixth Meeting, AGARD Rept. 507, June 1965, pp. 23-48.

11. Fradenburgh, Evan A.; and Wyatt, DeMarquis D.: Theoretical Performance Characteristics of Sharp-Lip Inlets at Subsonic Speeds. NACA Rept. 1193, 1954. (Supersedes NACA TN 3004.)

12. McLeod, Norman J.; Lasagna, Paul L.; and Putnam, Terrill W.: Predicted and Measured XB-70 Ground-to-Ground Engine Noise. Progress of NASA Research Relating to Noise Alleviation of Large Subsonic Jet Aircraft, NASA SP-189, 1968, pp. 423-434.

NASA-Langley, 1970 —— 28 H-578